Springer Series in
Computational
Mathematics

31

Ernst Hairer
Christian Lubich
Gerhard Wanner

Geometric Numerical Integration

Structure-Preserving Algorithms for Ordinary Differential Equations

Second Edition

With 146 Figures

Springer

Ernst Hairer
Gerhard Wanner
Section de Mathématiques
Université de Genève
2-4 rue du Lièvre, C.P. 64
CH-1211 Genève 4, Switzerland
email: Ernst.Hairer@math.unige.ch
Gerhard.Wanner@math.unige.ch

Christian Lubich
Mathematisches Institut
Universität Tübingen
Auf der Morgenstelle 10
72076 Tübingen, Germany
email: Lubich@na.uni-tuebingen.de

Library of Congress Control Number: 2005938386

Mathematics Subject Classification (2000): 65Lxx, 65P10, 70Fxx, 34Cxx

ISSN 0179-3632
ISBN-10 3-540-30663-3 Springer Berlin Heidelberg New York
ISBN-13 978-3-540-30663-4 Springer Berlin Heidelberg New York
ISBN-10 3-540-43003-2 1st Edition Springer Berlin Heidelberg New York

Springer is a part of Springer Science+Business Media
springer.com

Printed in The Netherlands

Typesetting: by the authors and TechBooks using a Springer LaTeX macro package

Cover design: *design & production* GmbH, Heidelberg

Printed on acid-free paper SPIN: 11592242 46/TechBooks 5 4 3 2 1 0

Preface to the First Edition

> They throw geometry out the door, and it comes back through the window.
> (H.G.Forder, Auckland 1973, reading new mathematics at the age of 84)

The subject of this book is numerical methods that preserve geometric properties of the flow of a differential equation: symplectic integrators for Hamiltonian systems, symmetric integrators for reversible systems, methods preserving first integrals and numerical methods on manifolds, including Lie group methods and integrators for constrained mechanical systems, and methods for problems with highly oscillatory solutions. Structure preservation – with its questions as to where, how, and what for – is the unifying theme.

In the last few decades, the theory of numerical methods for general (non-stiff and stiff) ordinary differential equations has reached a certain maturity, and excellent general-purpose codes, mainly based on Runge–Kutta methods or linear multistep methods, have become available. The motivation for developing structure-preserving algorithms for special classes of problems came independently from such different areas of research as astronomy, molecular dynamics, mechanics, theoretical physics, and numerical analysis as well as from other areas of both applied and pure mathematics. It turned out that the preservation of geometric properties of the flow not only produces an improved qualitative behaviour, but also allows for a more accurate long-time integration than with general-purpose methods.

An important shift of view-point came about by ceasing to concentrate on the numerical approximation of a single solution trajectory and instead to consider a numerical method as a *discrete dynamical system* which approximates the flow of the differential equation – and so the geometry of phase space comes back again through the window. This view allows a clear understanding of the preservation of invariants and of methods on manifolds, of symmetry and reversibility of methods, and of the symplecticity of methods and various generalizations. These subjects are presented in Chapters IV through VII of this book. Chapters I through III are of an introductory nature and present examples and numerical integrators together with important parts of the classical order theories and their recent extensions. Chapter VIII deals with questions of numerical implementations and numerical merits of the various methods.

It remains to explain the relationship between geometric properties of the numerical method and the favourable error propagation in long-time integrations. This

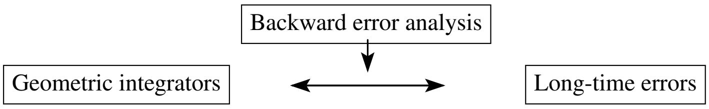

is done using the idea of *backward error analysis*, where the numerical one-step map is interpreted as (almost) the flow of a modified differential equation, which is constructed as an asymptotic series (Chapter IX). In this way, geometric properties of the numerical integrator translate into structure preservation on the level of the modified equations. Much insight and rigorous error estimates over long time intervals can then be obtained by combining this backward error analysis with KAM theory and related perturbation theories. This is explained in Chapters X through XII for Hamiltonian and reversible systems. The final Chapters XIII and XIV treat the numerical solution of differential equations with high-frequency oscillations and the long-time dynamics of multistep methods, respectively.

This book grew out of the lecture notes of a course given by Ernst Hairer at the University of Geneva during the academic year 1998/99. These lectures were directed at students in the third and fourth year. The reactions of students as well as of many colleagues, who obtained the notes from the Web, encouraged us to elaborate our ideas to produce the present monograph.

We want to thank all those who have helped and encouraged us to prepare this book. In particular, Martin Hairer for his valuable help in installing computers and his expertise in Latex and Postscript, Jeff Cash and Robert Chan for reading the whole text and correcting countless scientific obscurities and linguistic errors, Haruo Yoshida for making many valuable suggestions, Stéphane Cirilli for preparing the files for all the photographs, and Bernard Dudez, the irreplaceable director of the mathematics library in Geneva. We are also grateful to many friends and colleagues for reading parts of the manuscript and for valuable remarks and discussions, in particular to Assyr Abdulle, Melanie Beck, Sergio Blanes, John Butcher, Mari Paz Calvo, Begoña Cano, Philippe Chartier, David Cohen, Peter Deuflhard, Stig Faltinsen, Francesco Fassò, Martin Gander, Marlis Hochbruck, Bulent Karasözen, Wilhelm Kaup, Ben Leimkuhler, Pierre Leone, Frank Loose, Katina Lorenz, Robert McLachlan, Ander Murua, Alexander Ostermann, Truong Linh Pham, Sebastian Reich, Chus Sanz-Serna, Zaijiu Shang, Yifa Tang, Matt West, Will Wright.

We are especially grateful to Thanh-Ha Le Thi and Dr. Martin Peters from Springer-Verlag Heidelberg for assistance, in particular for their help in getting most of the original photographs from the Oberwolfach Archive and from Springer New York, and for clarifying doubts concerning the copyright.

Geneva and Tübingen, November 2001 The Authors

Preface to the Second Edition

The fast development of the subject – and the fast development of the sales of the first edition of this book – has given the authors the opportunity to prepare this second edition. First of all we have corrected several misprints and minor errors which we have discovered or which have been kindly communicated to us by several readers and colleagues. We cordially thank all of them for their help and for their interest in our work. A major point of confusion has been revealed by Robert McLachlan in his book review in SIAM Reviews.

Besides many details, which have improved the presentation throughout the book, there are the following major additions and changes which make the book about 130 pages longer:

- a more prominent place of the Störmer–Verlet method in the exposition and the examples of the first chapter;
- a discussion of the Hénon–Heiles model as an example of a chaotic Hamiltonian system;
- a new Sect. IV.9 on geometric numerical linear algebra considering differential equations on Stiefel and Grassmann manifolds and dynamical low-rank approximations;
- a new improved composition method of order 10 in Sect. V.3;
- a characterization of B-series methods that conserve quadratic first integrals and a criterion for conjugate symplecticity in Sect. VI.8;
- the section on volume preservation taken from Chap. VII to Chap. VI;
- an extended and more coherent Chap. VII, renamed Non-Canonical Hamiltonian Systems, with more emphasis on the relationships between Hamiltonian systems on manifolds and Poisson systems;
- a completely reorganized and augmented Sect. VII.5 on the rigid body dynamics and Lie–Poisson systems;
- a new Sect. VII.6 on reduced Hamiltonian models of quantum dynamics and Poisson integrators for their numerical treatment;
- an improved step-size control for reversible methods in Sects. VIII.3.2 and IX.6;
- extension of Sect. IX.5 on modified equations of methods on manifolds to include constrained Hamiltonian systems and Lie–Poisson integrators;
- reorganization of Sects. IX.9 and IX.10; study of non-symplectic B-series methods that have a modified Hamiltonian, and counter-examples for symmetric methods showing linear growth in the energy error;

- a more precise discussion of integrable reversible systems with new examples in Chap. XI;
- extension of Chap. XIII on highly oscillatory problems to systems with several constant frequencies and to systems with non-constant mass matrix;
- a new Chap. XIV on oscillatory Hamiltonian systems with time- or solution-dependent high frequencies, emphasizing adiabatic transformations, adiabatic invariants, and adiabatic integrators;
- a completely rewritten Chap. XV with more emphasis on linear multistep methods for second order differential equations; a complete backward error analysis including parasitic modified differential equations; a study of the long-time stability and a rigorous explanation of the long-time near-conservation of energy and angular momentum.

Let us hope that this second revised edition will again meet good acceptance by our readers.

Geneva and Tübingen, October 2005 The Authors

Table of Contents

I. Examples and Numerical Experiments 1
I.1 First Problems and Methods 1
I.1.1 The Lotka–Volterra Model 1
I.1.2 First Numerical Methods 3
I.1.3 The Pendulum as a Hamiltonian System 4
I.1.4 The Störmer–Verlet Scheme 7
I.2 The Kepler Problem and the Outer Solar System 8
I.2.1 Angular Momentum and Kepler's Second Law 9
I.2.2 Exact Integration of the Kepler Problem 10
I.2.3 Numerical Integration of the Kepler Problem 12
I.2.4 The Outer Solar System 13
I.3 The Hénon–Heiles Model 15
I.4 Molecular Dynamics 18
I.5 Highly Oscillatory Problems 21
I.5.1 A Fermi–Pasta–Ulam Problem 21
I.5.2 Application of Classical Integrators 23
I.6 Exercises 24

II. Numerical Integrators 27
II.1 Runge–Kutta and Collocation Methods 27
II.1.1 Runge–Kutta Methods 28
II.1.2 Collocation Methods 30
II.1.3 Gauss and Lobatto Collocation 34
II.1.4 Discontinuous Collocation Methods 35
II.2 Partitioned Runge–Kutta Methods 38
II.2.1 Definition and First Examples 38
II.2.2 Lobatto IIIA–IIIB Pairs 40
II.2.3 Nyström Methods 41
II.3 The Adjoint of a Method 42
II.4 Composition Methods 43
II.5 Splitting Methods 47
II.6 Exercises 50

III. Order Conditions, Trees and B-Series . . . 51
III.1 Runge–Kutta Order Conditions and B-Series . . . 51
III.1.1 Derivation of the Order Conditions . . . 51
III.1.2 B-Series . . . 56
III.1.3 Composition of Methods . . . 59
III.1.4 Composition of B-Series . . . 61
III.1.5 The Butcher Group . . . 64
III.2 Order Conditions for Partitioned Runge–Kutta Methods . . . 66
III.2.1 Bi-Coloured Trees and P-Series . . . 66
III.2.2 Order Conditions for Partitioned Runge–Kutta Methods 68
III.2.3 Order Conditions for Nyström Methods . . . 69
III.3 Order Conditions for Composition Methods . . . 71
III.3.1 Introduction . . . 71
III.3.2 The General Case . . . 73
III.3.3 Reduction of the Order Conditions . . . 75
III.3.4 Order Conditions for Splitting Methods . . . 80
III.4 The Baker-Campbell-Hausdorff Formula . . . 83
III.4.1 Derivative of the Exponential and Its Inverse . . . 83
III.4.2 The BCH Formula . . . 84
III.5 Order Conditions via the BCH Formula . . . 87
III.5.1 Calculus of Lie Derivatives . . . 87
III.5.2 Lie Brackets and Commutativity . . . 89
III.5.3 Splitting Methods . . . 91
III.5.4 Composition Methods . . . 92
III.6 Exercises . . . 95

IV. Conservation of First Integrals and Methods on Manifolds . . . 97
IV.1 Examples of First Integrals . . . 97
IV.2 Quadratic Invariants . . . 101
IV.2.1 Runge–Kutta Methods . . . 101
IV.2.2 Partitioned Runge–Kutta Methods . . . 102
IV.2.3 Nyström Methods . . . 104
IV.3 Polynomial Invariants . . . 105
IV.3.1 The Determinant as a First Integral . . . 105
IV.3.2 Isospectral Flows . . . 107
IV.4 Projection Methods . . . 109
IV.5 Numerical Methods Based on Local Coordinates . . . 113
IV.5.1 Manifolds and the Tangent Space . . . 114
IV.5.2 Differential Equations on Manifolds . . . 115
IV.5.3 Numerical Integrators on Manifolds . . . 116
IV.6 Differential Equations on Lie Groups . . . 118
IV.7 Methods Based on the Magnus Series Expansion . . . 121
IV.8 Lie Group Methods . . . 123
IV.8.1 Crouch-Grossman Methods . . . 124
IV.8.2 Munthe-Kaas Methods . . . 125

IV.8.3 Further Coordinate Mappings 128
IV.9 Geometric Numerical Integration Meets Geometric Numerical Linear Algebra 131
IV.9.1 Numerical Integration on the Stiefel Manifold 131
IV.9.2 Differential Equations on the Grassmann Manifold 135
IV.9.3 Dynamical Low-Rank Approximation 137
IV.10 Exercises 139

V. Symmetric Integration and Reversibility 143
V.1 Reversible Differential Equations and Maps 143
V.2 Symmetric Runge–Kutta Methods 146
V.2.1 Collocation and Runge–Kutta Methods 146
V.2.2 Partitioned Runge–Kutta Methods 148
V.3 Symmetric Composition Methods 149
V.3.1 Symmetric Composition of First Order Methods 150
V.3.2 Symmetric Composition of Symmetric Methods 154
V.3.3 Effective Order and Processing Methods 158
V.4 Symmetric Methods on Manifolds 161
V.4.1 Symmetric Projection 161
V.4.2 Symmetric Methods Based on Local Coordinates 166
V.5 Energy – Momentum Methods and Discrete Gradients 171
V.6 Exercises 176

VI. Symplectic Integration of Hamiltonian Systems 179
VI.1 Hamiltonian Systems 180
VI.1.1 Lagrange's Equations 180
VI.1.2 Hamilton's Canonical Equations 181
VI.2 Symplectic Transformations 182
VI.3 First Examples of Symplectic Integrators 187
VI.4 Symplectic Runge–Kutta Methods 191
VI.4.1 Criterion of Symplecticity 191
VI.4.2 Connection Between Symplectic and Symmetric Methods 194
VI.5 Generating Functions 195
VI.5.1 Existence of Generating Functions 195
VI.5.2 Generating Function for Symplectic Runge–Kutta Methods 198
VI.5.3 The Hamilton–Jacobi Partial Differential Equation 200
VI.5.4 Methods Based on Generating Functions 203
VI.6 Variational Integrators 204
VI.6.1 Hamilton's Principle 204
VI.6.2 Discretization of Hamilton's Principle 206
VI.6.3 Symplectic Partitioned Runge–Kutta Methods Revisited 208
VI.6.4 Noether's Theorem 210

VI.7 Characterization of Symplectic Methods 212
VI.7.1 B-Series Methods Conserving Quadratic First Integrals 212
VI.7.2 Characterization of Symplectic P-Series (and B-Series) 217
VI.7.3 Irreducible Runge–Kutta Methods 220
VI.7.4 Characterization of Irreducible Symplectic Methods . . . 222
VI.8 Conjugate Symplecticity 222
VI.8.1 Examples and Order Conditions 223
VI.8.2 Near Conservation of Quadratic First Integrals 225
VI.9 Volume Preservation 227
VI.10 Exercises 233

VII. Non-Canonical Hamiltonian Systems 237
VII.1 Constrained Mechanical Systems 237
VII.1.1 Introduction and Examples 237
VII.1.2 Hamiltonian Formulation 239
VII.1.3 A Symplectic First Order Method 242
VII.1.4 SHAKE and RATTLE 245
VII.1.5 The Lobatto IIIA - IIIB Pair 247
VII.1.6 Splitting Methods 252
VII.2 Poisson Systems 254
VII.2.1 Canonical Poisson Structure 254
VII.2.2 General Poisson Structures 256
VII.2.3 Hamiltonian Systems on Symplectic Submanifolds 258
VII.3 The Darboux–Lie Theorem 261
VII.3.1 Commutativity of Poisson Flows and Lie Brackets 261
VII.3.2 Simultaneous Linear Partial Differential Equations 262
VII.3.3 Coordinate Changes and the Darboux–Lie Theorem . . . 265
VII.4 Poisson Integrators 268
VII.4.1 Poisson Maps and Symplectic Maps 268
VII.4.2 Poisson Integrators 270
VII.4.3 Integrators Based on the Darboux–Lie Theorem 272
VII.5 Rigid Body Dynamics and Lie–Poisson Systems 274
VII.5.1 History of the Euler Equations 275
VII.5.2 Hamiltonian Formulation of Rigid Body Motion 278
VII.5.3 Rigid Body Integrators 280
VII.5.4 Lie–Poisson Systems 286
VII.5.5 Lie–Poisson Reduction 289
VII.6 Reduced Models of Quantum Dynamics 293
VII.6.1 Hamiltonian Structure of the Schrödinger Equation . . . 293
VII.6.2 The Dirac–Frenkel Variational Principle 295
VII.6.3 Gaussian Wavepacket Dynamics 296
VII.6.4 A Splitting Integrator for Gaussian Wavepackets 298
VII.7 Exercises 301

VIII. Structure-Preserving Implementation 303
VIII.1 Dangers of Using Standard Step Size Control 303
VIII.2 Time Transformations 306
VIII.2.1 Symplectic Integration 306
VIII.2.2 Reversible Integration 309
VIII.3 Structure-Preserving Step Size Control 310
VIII.3.1 Proportional, Reversible Controllers 310
VIII.3.2 Integrating, Reversible Controllers 314
VIII.4 Multiple Time Stepping 316
VIII.4.1 Fast-Slow Splitting: the Impulse Method 317
VIII.4.2 Averaged Forces 319
VIII.5 Reducing Rounding Errors 322
VIII.6 Implementation of Implicit Methods 325
VIII.6.1 Starting Approximations 326
VIII.6.2 Fixed-Point Versus Newton Iteration 330
VIII.7 Exercises 335

IX. Backward Error Analysis and Structure Preservation 337
IX.1 Modified Differential Equation – Examples 337
IX.2 Modified Equations of Symmetric Methods 342
IX.3 Modified Equations of Symplectic Methods 343
IX.3.1 Existence of a Local Modified Hamiltonian 343
IX.3.2 Existence of a Global Modified Hamiltonian 344
IX.3.3 Poisson Integrators 347
IX.4 Modified Equations of Splitting Methods 348
IX.5 Modified Equations of Methods on Manifolds 350
IX.5.1 Methods on Manifolds and First Integrals 350
IX.5.2 Constrained Hamiltonian Systems 352
IX.5.3 Lie–Poisson Integrators 354
IX.6 Modified Equations for Variable Step Sizes 356
IX.7 Rigorous Estimates – Local Error 358
IX.7.1 Estimation of the Derivatives of the Numerical Solution 360
IX.7.2 Estimation of the Coefficients of the Modified Equation 362
IX.7.3 Choice of N and the Estimation of the Local Error 364
IX.8 Long-Time Energy Conservation 366
IX.9 Modified Equation in Terms of Trees 369
IX.9.1 B-Series of the Modified Equation 369
IX.9.2 Elementary Hamiltonians 373
IX.9.3 Modified Hamiltonian 375
IX.9.4 First Integrals Close to the Hamiltonian 375
IX.9.5 Energy Conservation: Examples and Counter-Examples 379
IX.10 Extension to Partitioned Systems 381
IX.10.1 P-Series of the Modified Equation 381
IX.10.2 Elementary Hamiltonians 384
IX.11 Exercises 386

X. Hamiltonian Perturbation Theory and Symplectic Integrators 389
X.1 Completely Integrable Hamiltonian Systems 390
X.1.1 Local Integration by Quadrature 390
X.1.2 Completely Integrable Systems 393
X.1.3 Action-Angle Variables 397
X.1.4 Conditionally Periodic Flows 399
X.1.5 The Toda Lattice – an Integrable System 402
X.2 Transformations in the Perturbation Theory for Integrable Systems 404
X.2.1 The Basic Scheme of Classical Perturbation Theory . . . 405
X.2.2 Lindstedt–Poincaré Series 406
X.2.3 Kolmogorov's Iteration 410
X.2.4 Birkhoff Normalization Near an Invariant Torus 412
X.3 Linear Error Growth and Near-Preservation of First Integrals . . . 413
X.4 Near-Invariant Tori on Exponentially Long Times 417
X.4.1 Estimates of Perturbation Series 417
X.4.2 Near-Invariant Tori of Perturbed Integrable Systems . . . 421
X.4.3 Near-Invariant Tori of Symplectic Integrators 422
X.5 Kolmogorov's Theorem on Invariant Tori 423
X.5.1 Kolmogorov's Theorem 423
X.5.2 KAM Tori under Symplectic Discretization 428
X.6 Invariant Tori of Symplectic Maps 430
X.6.1 A KAM Theorem for Symplectic Near-Identity Maps . 431
X.6.2 Invariant Tori of Symplectic Integrators 433
X.6.3 Strongly Non-Resonant Step Sizes 433
X.7 Exercises 434

XI. Reversible Perturbation Theory and Symmetric Integrators 437
XI.1 Integrable Reversible Systems 437
XI.2 Transformations in Reversible Perturbation Theory 442
XI.2.1 The Basic Scheme of Reversible Perturbation Theory . . 443
XI.2.2 Reversible Perturbation Series 444
XI.2.3 Reversible KAM Theory 445
XI.2.4 Reversible Birkhoff-Type Normalization 447
XI.3 Linear Error Growth and Near-Preservation of First Integrals . . . 448
XI.4 Invariant Tori under Reversible Discretization 451
XI.4.1 Near-Invariant Tori over Exponentially Long Times . . . 451
XI.4.2 A KAM Theorem for Reversible Near-Identity Maps . . 451
XI.5 Exercises 453

XII. Dissipatively Perturbed Hamiltonian and Reversible Systems 455
XII.1 Numerical Experiments with Van der Pol's Equation 455
XII.2 Averaging Transformations 458
XII.2.1 The Basic Scheme of Averaging 458
XII.2.2 Perturbation Series 459

XII.3 Attractive Invariant Manifolds 460
XII.4 Weakly Attractive Invariant Tori of Perturbed Integrable Systems 464
XII.5 Weakly Attractive Invariant Tori of Numerical Integrators 465
XII.5.1 Modified Equations of Perturbed Differential Equations 466
XII.5.2 Symplectic Methods 467
XII.5.3 Symmetric Methods 469
XII.6 Exercises 469

XIII. Oscillatory Differential Equations with Constant High Frequencies . 471
XIII.1 Towards Longer Time Steps in Solving Oscillatory Equations of Motion 471
XIII.1.1 The Störmer–Verlet Method vs. Multiple Time Scales . 472
XIII.1.2 Gautschi's and Deuflhard's Trigonometric Methods . . . 473
XIII.1.3 The Impulse Method 475
XIII.1.4 The Mollified Impulse Method 476
XIII.1.5 Gautschi's Method Revisited 477
XIII.1.6 Two-Force Methods 478
XIII.2 A Nonlinear Model Problem and Numerical Phenomena 478
XIII.2.1 Time Scales in the Fermi–Pasta–Ulam Problem 479
XIII.2.2 Numerical Methods 481
XIII.2.3 Accuracy Comparisons 482
XIII.2.4 Energy Exchange between Stiff Components 483
XIII.2.5 Near-Conservation of Total and Oscillatory Energy 484
XIII.3 Principal Terms of the Modulated Fourier Expansion 486
XIII.3.1 Decomposition of the Exact Solution 486
XIII.3.2 Decomposition of the Numerical Solution 488
XIII.4 Accuracy and Slow Exchange 490
XIII.4.1 Convergence Properties on Bounded Time Intervals . . . 490
XIII.4.2 Intra-Oscillatory and Oscillatory-Smooth Exchanges . . 494
XIII.5 Modulated Fourier Expansions 496
XIII.5.1 Expansion of the Exact Solution 496
XIII.5.2 Expansion of the Numerical Solution 498
XIII.5.3 Expansion of the Velocity Approximation 502
XIII.6 Almost-Invariants of the Modulated Fourier Expansions 503
XIII.6.1 The Hamiltonian of the Modulated Fourier Expansion . 503
XIII.6.2 A Formal Invariant Close to the Oscillatory Energy . . . 505
XIII.6.3 Almost-Invariants of the Numerical Method 507
XIII.7 Long-Time Near-Conservation of Total and Oscillatory Energy . 510
XIII.8 Energy Behaviour of the Störmer–Verlet Method 513
XIII.9 Systems with Several Constant Frequencies 516
XIII.9.1 Oscillatory Energies and Resonances 517
XIII.9.2 Multi-Frequency Modulated Fourier Expansions 519
XIII.9.3 Almost-Invariants of the Modulation System 521
XIII.9.4 Long-Time Near-Conservation of Total and Oscillatory Energies 524

XIII.10 Systems with Non-Constant Mass Matrix . . . 526
XIII.11 Exercises . . . 529

XIV. Oscillatory Differential Equations with Varying High Frequencies . . 531
XIV.1 Linear Systems with Time-Dependent Skew-Hermitian Matrix . . 531
XIV.1.1 Adiabatic Transformation and Adiabatic Invariants . . . 531
XIV.1.2 Adiabatic Integrators . . . 536
XIV.2 Mechanical Systems with Time-Dependent Frequencies . . . 539
XIV.2.1 Canonical Transformation to Adiabatic Variables . . . 540
XIV.2.2 Adiabatic Integrators . . . 547
XIV.2.3 Error Analysis of the Impulse Method . . . 550
XIV.2.4 Error Analysis of the Mollified Impulse Method . . . 554
XIV.3 Mechanical Systems with Solution-Dependent Frequencies . . . 555
XIV.3.1 Constraining Potentials . . . 555
XIV.3.2 Transformation to Adiabatic Variables . . . 558
XIV.3.3 Integrators in Adiabatic Variables . . . 563
XIV.3.4 Analysis of Multiple Time-Stepping Methods . . . 564
XIV.4 Exercises . . . 564

XV. Dynamics of Multistep Methods . . . 567
XV.1 Numerical Methods and Experiments . . . 567
XV.1.1 Linear Multistep Methods . . . 567
XV.1.2 Multistep Methods for Second Order Equations . . . 569
XV.1.3 Partitioned Multistep Methods . . . 572
XV.2 The Underlying One-Step Method . . . 573
XV.2.1 Strictly Stable Multistep methods . . . 573
XV.2.2 Formal Analysis for Weakly Stable Methods . . . 575
XV.3 Backward Error Analysis . . . 576
XV.3.1 Modified Equation for Smooth Numerical Solutions . . . 576
XV.3.2 Parasitic Modified Equations . . . 579
XV.4 Can Multistep Methods be Symplectic? . . . 585
XV.4.1 Non-Symplecticity of the Underlying One-Step Method 585
XV.4.2 Symplecticity in the Higher-Dimensional Phase Space . 587
XV.4.3 Modified Hamiltonian of Multistep Methods . . . 589
XV.4.4 Modified Quadratic First Integrals . . . 591
XV.5 Long-Term Stability . . . 592
XV.5.1 Role of Growth Parameters . . . 592
XV.5.2 Hamiltonian of the Full Modified System . . . 594
XV.5.3 Long-Time Bounds for Parasitic Solution Components 596
XV.6 Explanation of the Long-Time Behaviour . . . 600
XV.6.1 Conservation of Energy and Angular Momentum . . . 600
XV.6.2 Linear Error Growth for Integrable Systems . . . 601
XV.7 Practical Considerations . . . 602
XV.7.1 Numerical Instabilities and Resonances . . . 602
XV.7.2 Extension to Variable Step Sizes . . . 605

XV.8 Multi-Value or General Linear Methods . . . 609
XV.8.1 Underlying One-Step Method and Backward Error Analysis . . . 609
XV.8.2 Symplecticity and Symmetry . . . 611
XV.8.3 Growth Parameters . . . 614
XV.9 Exercises . . . 615

Bibliography . . . 617

Index . . . 637

Chapter I.
Examples and Numerical Experiments

This chapter introduces some interesting examples of differential equations and illustrates different types of qualitative behaviour of numerical methods. We deliberately consider only very simple numerical methods of orders 1 and 2 to emphasize the qualitative aspects of the experiments. The same effects (on a different scale) occur with more sophisticated higher-order integration schemes. The experiments presented here should serve as a motivation for the theoretical and practical investigations of later chapters. The reader is encouraged to repeat the experiments or to invent similar ones.

I.1 First Problems and Methods

> Numerical applications of the case of two dependent variables are not easily obtained. (A.J. Lotka 1925, p. 79)

Our first problems, the Lotka–Volterra model and the pendulum equation, are differential equations in two dimensions and show already many interesting geometric properties. Our first methods are various variants of the Euler method, the midpoint rule, and the Störmer–Verlet scheme.

I.1.1 The Lotka–Volterra Model

We start with an equation from mathematical biology which models the growth of animal species. If a real variable $u(t)$ is to represent the number of individuals of a certain species at time t, the simplest assumption about its evolution is $du/dt = u\cdot\alpha$, where α is the reproduction rate. A constant α leads to exponential growth. In the case of more species living together, the reproduction rates will also depend on the population numbers of the *other* species. For example, for two species with $u(t)$ denoting the number of predators and $v(t)$ the number of prey, a plausible assumption is made by the *Lotka–Volterra model*

$$\begin{aligned} \dot u &= u(v-2) \\ \dot v &= v(1-u), \end{aligned} \tag{1.1}$$

where the dots on u and v stand for differentiation with respect to time. (We have chosen the constants 2 and 1 in (1.1) arbitrarily.) A.J. Lotka (1925, Chap. VIII) used

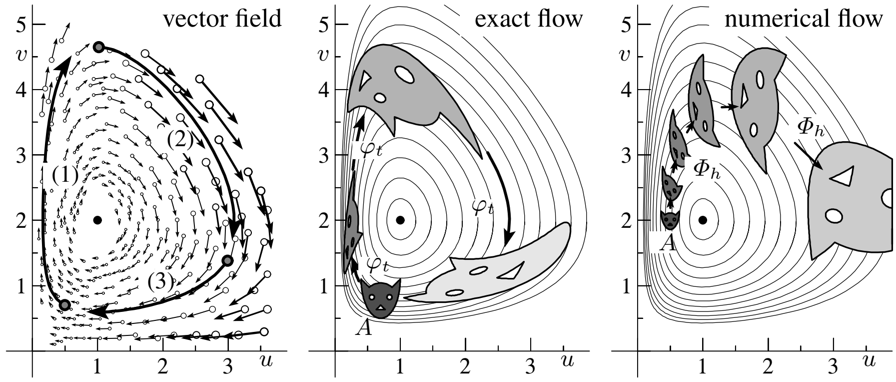

Fig. 1.1. Vector field, exact flow, and numerical flow for the Lotka–Volterra model (1.1)

this model to study parasitic invasion of insect species, and, with its help, V. Volterra (1927) explained curious fishing data from the upper Adriatic Sea following World War I.

Equations (1.1) constitute an autonomous system of differential equations. In general, we write such a system in the form

$$\dot{y} = f(y)\ . \tag{1.2}$$

Every y represents a point in the *phase space*, in equation (1.1) above $y = (u, v)$ is in the phase plane $\mathbb{R}^2$. The vector-valued function $f(y)$ represents a *vector field* which, at any point of the phase space, prescribes the velocity (direction and speed) of the solution $y(t)$ that passes through that point (see the first picture of Fig. 1.1).

For the Lotka–Volterra model, we observe that the system cycles through three stages: (1) the prey population increases; (2) the predator population increases by feeding on the prey; (3) the predator population diminishes due to lack of food.

Flow of the System. A fundamental concept is the *flow* over time t. This is the mapping which, to any point y_0 in the phase space, associates the value $y(t)$ of the solution with initial value $y(0) = y_0$. This map, denoted by φ_t, is thus defined by

$$\varphi_t(y_0) = y(t) \quad \text{if} \quad y(0) = y_0. \tag{1.3}$$

The second picture of Fig. 1.1 shows the results of three iterations of φ_t (with $t = 1.3$) for the Lotka–Volterra problem, for a set of initial values $y_0 = (u_0, v_0)$ forming an animal-shaped set A.[1]

Invariants. If we divide the two equations of (1.1) by each other, we obtain a single equation between the variables u and v. After separation of variables we get

$$0 = \frac{1-u}{u}\,\dot{u} - \frac{v-2}{v}\,\dot{v} = \frac{d}{dt}\,I(u, v)$$

[1] This cat came to fame through Arnold (1963).

where

$$I(u,v) = \ln u - u + 2\ln v - v, \tag{1.4}$$

so that $I(u(t),v(t)) = \mathit{Const}$ for all t. We call the function I an *invariant* of the system (1.1). Every solution of (1.1) thus lies on a level curve of (1.4). Some of these curves are drawn in the pictures of Fig. 1.1. Since the level curves are closed, all solutions of (1.1) are periodic.

I.1.2 First Numerical Methods

Explicit Euler Method. The simplest of all numerical methods for the system (1.2) is the method formulated by Euler (1768),

$$y_{n+1} = y_n + hf(y_n). \tag{1.5}$$

It uses a constant step size h to compute, one after the other, approximations y_1, y_2, y_3, ... to the values $y(h)$, $y(2h)$, $y(3h)$, ... of the solution starting from a given initial value $y(0) = y_0$. The method is called the *explicit Euler method*, because the approximation y_{n+1} is computed using an explicit evaluation of f at the already known value y_n. Such a formula represents a mapping

$$\Phi_h : y_n \mapsto y_{n+1},$$

which we call the *discrete* or *numerical flow*. Some iterations of the discrete flow for the Lotka–Volterra problem (1.1) (with $h = 0.5$) are represented in the third picture of Fig. 1.1.

Implicit Euler Method. The *implicit Euler method*

$$y_{n+1} = y_n + hf(y_{n+1}), \tag{1.6}$$

is known for its all-damping stability properties. In contrast to (1.5), the approximation y_{n+1} is defined implicitly by (1.6), and the implementation requires the numerical solution of a nonlinear system of equations.

Implicit Midpoint Rule. Taking the mean of y_n and y_{n+1} in the argument of f, we get the *implicit midpoint rule*

$$y_{n+1} = y_n + hf\Big(\frac{y_n + y_{n+1}}{2}\Big). \tag{1.7}$$

It is a *symmetric* method, which means that the formula is left unaltered after exchanging $y_n \leftrightarrow y_{n+1}$ and $h \leftrightarrow -h$ (more on symmetric methods in Chap. V).

Symplectic Euler Methods. For *partitioned* systems

$$\begin{aligned} \dot u &= a(u,v) \\ \dot v &= b(u,v), \end{aligned} \tag{1.8}$$

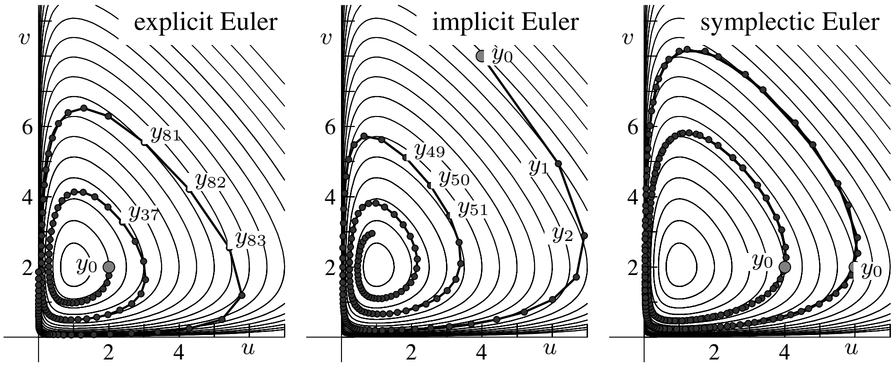

Fig. 1.2. Solutions of the Lotka–Volterra equations (1.1) (step sizes $h = 0.12$; initial values $(2,2)$ for the explicit Euler method, $(4,8)$ for the implicit Euler method, $(4,2)$ and $(6,2)$ for the symplectic Euler method)

such as the problem (1.1), we consider also *partitioned* Euler methods

$$\begin{aligned} u_{n+1} &= u_n + ha(u_n, v_{n+1}) \\ v_{n+1} &= v_n + hb(u_n, v_{n+1}), \end{aligned} \quad \text{or} \quad \begin{aligned} u_{n+1} &= u_n + ha(u_{n+1}, v_n) \\ v_{n+1} &= v_n + hb(u_{n+1}, v_n), \end{aligned} \tag{1.9}$$

which treat one variable by the implicit and the other variable by the explicit Euler method. In view of an important property of this method, discovered by de Vogelaere (1956) and to be discussed in Chap. VI, we call them *symplectic Euler methods*.

Numerical Example for the Lotka–Volterra Problem. Our first numerical experiment shows the behaviour of the various numerical methods applied to the Lotka–Volterra problem. In particular, we are interested in the preservation of the invariant I over long times. Fig. 1.2 plots the numerical approximations of the first 125 steps with the above numerical methods applied to (1.1), all with constant step sizes. We observe that the explicit and implicit Euler methods show wrong qualitative behaviour. The numerical solution either spirals outwards or inwards. The symplectic Euler method (implicit in u and explicit in v), however, gives a numerical solution that lies apparently on a closed curve as does the exact solution. Note that the curves of the numerical and exact solutions do not coincide.

I.1.3 The Pendulum as a Hamiltonian System

A great deal of attention in this book will be addressed to Hamiltonian problems, and our next examples will be of this type. These problems are of the form

$$\dot{p} = -H_q(p,q), \qquad \dot{q} = H_p(p,q), \tag{1.10}$$

where the *Hamiltonian* $H(p_1,\ldots,p_d,q_1,\ldots q_d)$ represents the total energy; q_i are the position coordinates and p_i the momenta for $i = 1,\ldots,d$, with d the number of degrees of freedom; H_p and H_q are the vectors of partial derivatives. One verifies easily by differentiation (see Sect. IV.1) that, along the solution curves of (1.10),

$$H\big(p(t), q(t)\big) = Const, \tag{1.11}$$

i.e., the Hamiltonian is an invariant or a *first integral*. More details about Hamiltonian systems and their derivation from Lagrangian mechanics will be given in Sect. VI.1.

Pendulum. The mathematical pendulum (mass $m = 1$, massless rod of length $\ell = 1$, gravitational acceleration $g = 1$) is a system with one degree of freedom having the Hamiltonian

$$H(p, q) = \frac{1}{2}\,p^2 - \cos q, \tag{1.12}$$

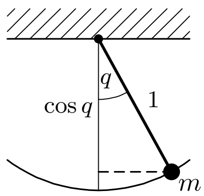

so that the equations of motion (1.10) become

$$\dot p = -\sin q, \qquad \dot q = p. \tag{1.13}$$

Since the vector field (1.13) is 2π-periodic in q, it is natural to consider q as a variable on the circle S^1. Hence, the phase space of points (p, q) becomes the cylinder $\mathbb{R} \times S^1$. Fig. 1.3 shows some level curves of $H(p, q)$. By (1.11), the solution curves of the problem (1.13) lie on such level curves.

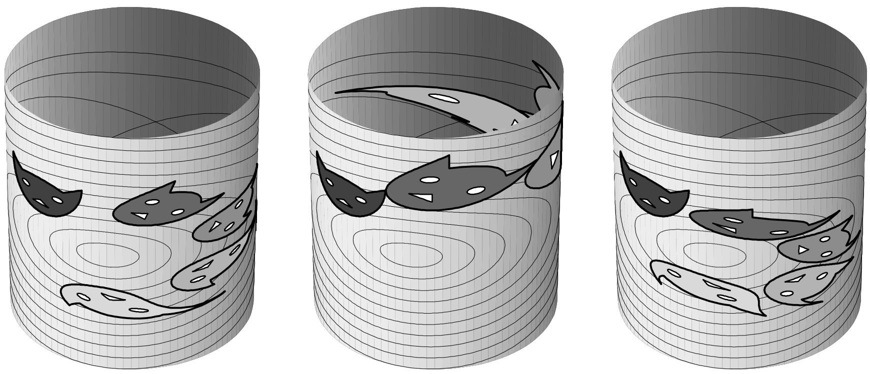

Fig. 1.3. Exact and numerical flow for the pendulum problem (1.13); step sizes $h = t = 1$

Area Preservation. Figure 1.3 (first picture) illustrates that the exact flow of a Hamiltonian system (1.10) is area preserving. This can be explained as follows: the derivative of the flow φ_t with respect to initial values (p, q),

$$\varphi_t'(p, q) = \frac{\partial\big(p(t), q(t)\big)}{\partial(p, q)},$$

satisfies the variational equation [2]

$$\dot{\varphi}'_t(p,q) = \begin{pmatrix} -H_{pq} & -H_{qq} \\ H_{pp} & H_{qp} \end{pmatrix} \varphi'_t(p,q) \ ,$$

where the second partial derivatives of H are evaluated at $\varphi_t(p,q)$. In the case of one degree of freedom ($d=1$), a simple computation shows that

$$\frac{d}{dt} \det \varphi'_t(p,q) = \frac{d}{dt}\Big(\frac{\partial p(t)}{\partial p}\,\frac{\partial q(t)}{\partial q} - \frac{\partial p(t)}{\partial q}\,\frac{\partial q(t)}{\partial p} \Big) = \ldots = 0.$$

Since φ_0 is the identity, this implies $\det \varphi'_t(p,q) = 1$ for all t, which means that the flow $\varphi_t(p,q)$ is an *area-preserving* mapping.

The last two pictures of Fig. 1.3 show numerical flows. The explicit Euler method is clearly seen not to preserve area but the symplectic Euler method is (this will be proved in Sect. VI.3). One of the aims of 'geometric integration' is the study of numerical integrators that preserve such types of qualitative behaviour of the exact flow.

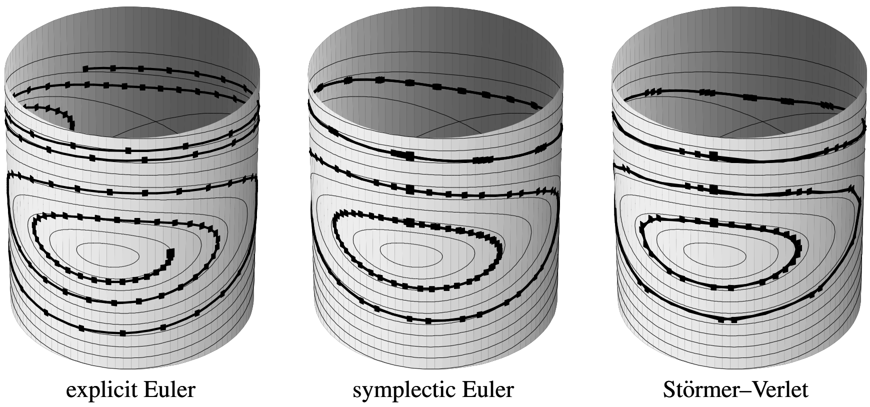

Fig. 1.4. Solutions of the pendulum problem (1.13); explicit Euler with step size $h = 0.2$, initial value $(p_0, q_0) = (0, 0.5)$; symplectic Euler with $h = 0.3$ and initial values $q_0 = 0$, $p_0 = 0.7, 1.4, 2.1$; Störmer–Verlet with $h = 0.6$

Numerical Experiment. We apply the above numerical methods to the pendulum equations (see Fig. 1.4). Similar to the computations for the Lotka–Volterra equations, we observe that the numerical solutions of the explicit Euler and of the implicit Euler method (not drawn in Fig. 1.4) spiral either outwards or inwards. The symplectic Euler method shows the correct qualitative behaviour, but destroys the left-right symmetry of the problem. The Störmer–Verlet scheme, which we discuss next, works perfectly even with doubled step size.

[2] As is common in the study of mechanical problems, we use *dots* for denoting time-derivatives, and we use *primes* for denoting derivatives with respect to other variables.

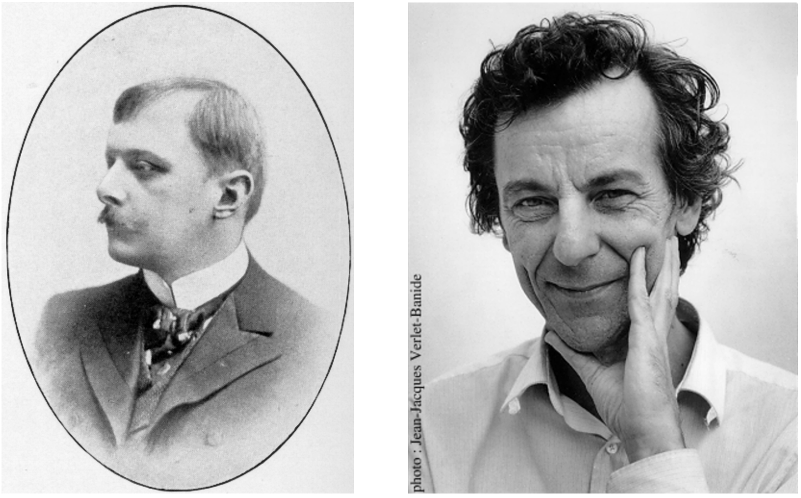

Fig. 1.5. Carl Störmer (left picture), born: 3 September 1874 in Skien (Norway), died: 13 August 1957.
Loup Verlet (right picture), born: 24 May 1931 in Paris

I.1.4 The Störmer–Verlet Scheme

The above equations (1.13) for the pendulum are of the form

$$\begin{aligned} \dot{p} &= f(q) \\ \dot{q} &= p \end{aligned} \qquad \text{or} \qquad \ddot{q} = f(q) \tag{1.14}$$

which is the important special case of a second order differential equation. The most natural discretization of (1.14) is

$$q_{n+1} - 2q_n + q_{n-1} = h^2 f(q_n), \tag{1.15}$$

which is just obtained by replacing the second derivative in (1.14) by the central second-order difference quotient. This basic method, or its equivalent formulation given below, is called the *Störmer method* in astronomy, the *Verlet method* [3] in molecular dynamics, the *leap-frog method* in the context of partial differential equations, and it has further names in other areas (see Hairer, Lubich & Wanner (2003), p. 402). C. Störmer (1907) used higher-order variants for numerical computations concerning the aurora borealis. L. Verlet (1967) proposed this method for computations in molecular dynamics, where it has become by far the most widely used integration scheme.

Geometrically, the Störmer–Verlet method can be seen as produced by parabolas, which in the points t_n possess the right second derivative $f(q_n)$ (see Fig. 1.6

[3] Irony of fate: Professor Loup Verlet, who later became interested in the history of science, discovered precisely “his” method in Newton’s *Principia* (Book I, figure for Theorem I, see Sect. I.2.1 below).

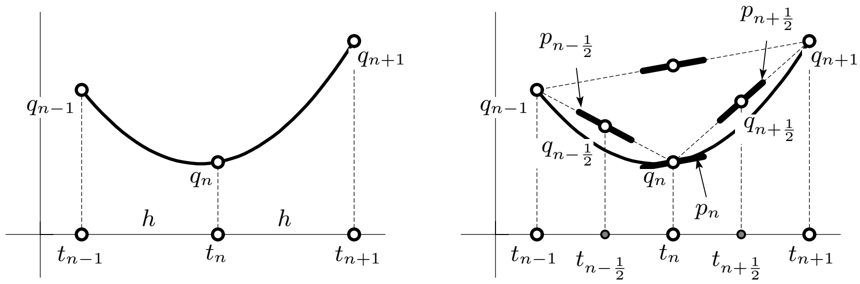

Fig. 1.6. Illustration for the Störmer–Verlet method

to the left). But we can also think of polygons, which possess the right slope in the midpoints (Fig. 1.6 to the right).

Approximations to the derivative $p = \dot{q}$ are simply obtained by

$$p_n = \frac{q_{n+1} - q_{n-1}}{2h} \qquad \text{and} \qquad p_{n+1/2} = \frac{q_{n+1} - q_n}{h}. \tag{1.16}$$

One-Step Formulation. The Störmer–Verlet method admits a one-step formulation which is useful for actual computations. The value q_n together with the slope p_n and the second derivative $f(q_n)$, all at t_n, uniquely determine the parabola and hence also the approximation (p_{n+1}, q_{n+1}) at t_{n+1}. Writing (1.15) as $p_{n+1/2} - p_{n-1/2} = hf(q_n)$ and using $p_{n+1/2} + p_{n-1/2} = 2p_n$, we get by elimination of either $p_{n+1/2}$ or $p_{n-1/2}$ the formulae

$$\begin{aligned} p_{n+1/2} &= p_n + \frac{h}{2} f(q_n) \\ q_{n+1} &= q_n + hp_{n+1/2} \\ p_{n+1} &= p_{n+1/2} + \frac{h}{2} f(q_{n+1}) \end{aligned} \tag{1.17}$$

which is an explicit one-step method $\Phi_h : (q_n, p_n) \mapsto (q_{n+1}, p_{n+1})$ for the corresponding first order system of (1.14). If one is not interested in the values p_n of the derivative, the first and third equations in (1.17) can be replaced by

$$p_{n+1/2} = p_{n-1/2} + h\, f(q_n).$$

I.2 The Kepler Problem and the Outer Solar System

I awoke as if from sleep, a new light broke on me. (J. Kepler; quoted from J.L.E. Dreyer, *A history of astronomy*, 1906, Dover 1953, p. 391)

One of the great achievements in the history of science was the discovery of the laws of J. Kepler (1609), based on many precise measurements of the positions of Mars by Tycho Brahe and himself. The planets move in *elliptic orbits* with the sun at one of the foci (Kepler's first law)

$$r = \frac{d}{1 + e\cos\varphi} = a - ae\cos E, \tag{2.1}$$

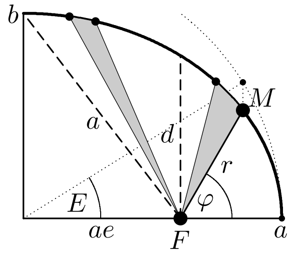

(where a = great axis, e = eccentricity, $b = a\sqrt{1-e^2}$, $d = b\sqrt{1-e^2} = a(1-e^2)$, E = eccentric anomaly, φ = true anomaly).

Newton (*Principia* 1687) then *explained* this motion by his general law of gravitational attraction (proportional to $1/r^2$) and the relation between forces and acceleration (the "Lex II" of the *Principia*). This then opened the way for treating arbitrary celestial motions by solving differential equations.

Two-Body Problem. For computing the motion of two bodies which attract each other, we choose one of the bodies as the centre of our coordinate system; the motion will then stay in a plane (Exercise 3) and we can use two-dimensional coordinates $q = (q_1, q_2)$ for the position of the second body. Newton's laws, with a suitable normalization, then yield the following differential equations

$$\ddot{q}_1 = -\frac{q_1}{(q_1^2 + q_2^2)^{3/2}}, \qquad \ddot{q}_2 = -\frac{q_2}{(q_1^2 + q_2^2)^{3/2}}. \tag{2.2}$$

This is equivalent to a Hamiltonian system with the Hamiltonian

$$H(p_1, p_2, q_1, q_2) = \frac{1}{2}\left(p_1^2 + p_2^2\right) - \frac{1}{\sqrt{q_1^2 + q_2^2}}, \qquad p_i = \dot{q}_i. \tag{2.3}$$

I.2.1 Angular Momentum and Kepler's Second Law

The system has not only the total energy $H(p,q)$ as a first integral, but also the angular momentum

$$L(p_1, p_2, q_1, q_2) = q_1 p_2 - q_2 p_1. \tag{2.4}$$

This can be checked by differentiation and is nothing other than *Kepler's second law*, which says that the ray FM sweeps equal areas in equal times (see the little picture at the beginning of Sect. I.2).

A beautiful *geometric* justification of this law is due to I. Newton[4] (*Principia* (1687), Book I, figure for Theorem I). The idea is to apply the Störmer–Verlet scheme (1.15) to the equations (2.2) (see Fig. 2.1). By hypothesis, the diagonal of the parallelogram $q_{n-1}q_n q_{n+1}$, which is $(q_{n+1} - q_n) - (q_n - q_{n-1}) = q_{n+1} - 2q_n + q_{n-1} = Const \cdot f(q_n)$, points towards the sun S. Therefore, the altitudes of the triangles $q_{n-1}q_n S$ and $q_{n+1}q_n S$ are equal. Since they have the common base $q_n S$, they also have equal areas. Hence

$$\det(q_{n-1}, q_n - q_{n-1}) = \det(q_n, q_{n+1} - q_n)$$

and by passing to the limit $h \to 0$ we see that $\det(q,p) = Const$. This is (2.4).

[4] We are grateful to a private communication of L. Verlet for this reference

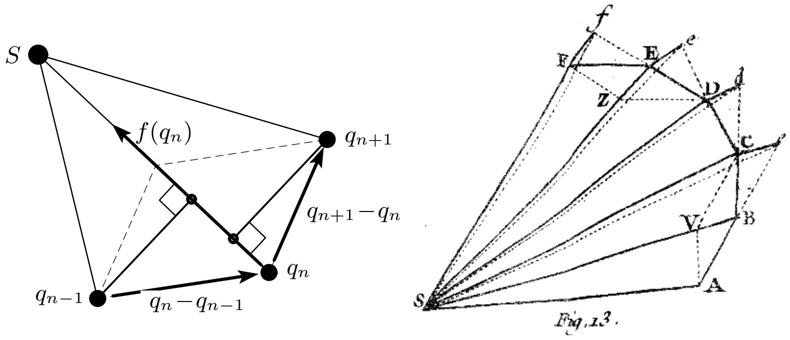

Fig. 2.1. Proof of Kepler's Second Law (left); facsimile from Newton's *Principia* (right)

We have not only an elegant proof for this invariant, but we also see that *the Störmer–Verlet scheme preserves this invariant for every* $h > 0$.

I.2.2 Exact Integration of the Kepler Problem

> Pour voir présentement que cette courbe ABC ... est toûjours une Section Conique, ainsi que Mr. Newton l'a supposé, *pag. 55. Coroll.I.* sans le démontrer; il y faut bien plus d'adresse: (Joh. Bernoulli 1710, p. 475)

It is now interesting, inversely to the procedure of Newton, to prove that *any* solution of (2.2) follows either an elliptic, parabolic or hyperbolic arc and to describe the solutions analytically. This was first done by Joh. Bernoulli (1710, full of sarcasm against Newton), and by Newton (1713, second edition of the *Principia*, without mentioning a word about Bernoulli).

By (2.3) and (2.4), every solution of (2.2) satisfies the two relations

$$\frac{1}{2}\left(\dot{q}_1^2+\dot{q}_2^2\right)-\frac{1}{\sqrt{q_1^2+q_2^2}}=H_0, \qquad q_1\dot{q}_2-q_2\dot{q}_1=L_0, \tag{2.5}$$

where the constants H_0 and L_0 are determined by the initial values. Using polar coordinates $q_1 = r\cos\varphi$, $q_2 = r\sin\varphi$, this system becomes

$$\frac{1}{2}\left(\dot{r}^2+r^2\dot{\varphi}^2\right)-\frac{1}{r}=H_0, \qquad r^2\dot{\varphi}=L_0. \tag{2.6}$$

For its solution we consider r as a function of φ and write $\dot{r}=\frac{dr}{d\varphi}\cdot\dot{\varphi}$. The elimination of $\dot{\varphi}$ in (2.6) then yields

$$\frac{1}{2}\left(\left(\frac{dr}{d\varphi}\right)^2+r^2\right)\frac{L_0^2}{r^4}-\frac{1}{r}=H_0.$$

In this equation we use the substitution $r = 1/u$, $dr = -du/u^2$, which gives (with $' = d/d\varphi$)

$$\frac{1}{2}(u'^2+u^2)-\frac{u}{L_0^2}-\frac{H_0}{L_0^2}=0. \tag{2.7}$$

This is a "Hamiltonian" for the system

$$u'' + u = \frac{1}{d} \quad \text{i.e.,} \quad u = \frac{1}{d} + c_1 \cos\varphi + c_2 \sin\varphi = \frac{1 + e\cos(\varphi - \varphi^*)}{d} \tag{2.8}$$

where $d = L_0^2$ and the constant e becomes, from (2.7),

$$e^2 = 1 + 2H_0 L_0^2 \tag{2.9}$$

(by Exercise 7, the expression $1+2H_0L_0^2$ is non-negative). This is precisely formula (2.1). The angle φ^* is determined by the initial values r_0 and φ_0. Equation (2.1) represents an elliptic orbit with eccentricity e for $H_0 < 0$ (see Fig. 2.2, dotted line), a parabola for $H_0 = 0$, and a hyperbola for $H_0 > 0$.

Finally, we must determine the variables r and φ as functions of t. With the relation (2.8) and $r = 1/u$, the second equation of (2.6) gives

$$\frac{d^2}{\big(1 + e\cos(\varphi - \varphi^*)\big)^2}\, d\varphi = L_0\, dt \tag{2.10}$$

which, after an elementary, but not easy, integration, represents an implicit equation for $\varphi(t)$.

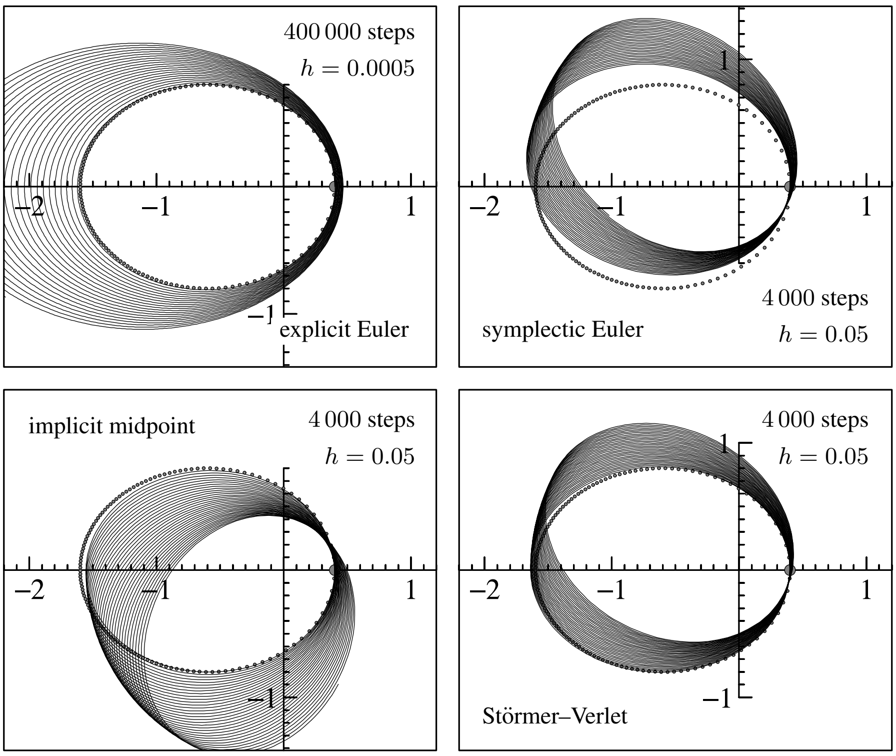

Fig. 2.2. Numerical solutions of the Kepler problem (eccentricity $e = 0.6$; in dots: exact solution)

I.2.3 Numerical Integration of the Kepler Problem

For the problem (2.2) we choose, with $0 \le e < 1$, the initial values

$$q_1(0) = 1 - e, \quad q_2(0) = 0, \quad \dot{q}_1(0) = 0, \quad \dot{q}_2(0) = \sqrt{\frac{1+e}{1-e}}. \qquad (2.11)$$

This implies that $H_0 = -1/2$, $L_0 = \sqrt{1-e^2}$, $d = 1 - e^2$ and $\varphi^* = 0$. The period of the solution is 2π (Exercise 5). Fig. 2.2 shows some numerical solutions for the eccentricity $e = 0.6$ compared to the exact solution. After our previous experience, it is no longer a surprise that the explicit Euler method spirals outwards and gives a completely wrong answer. For the other methods we take a step size 100 times larger in order to "see something". We see that the nonsymmetric symplectic Euler method distorts the ellipse, and that all methods exhibit a *precession* effect, clockwise for Störmer–Verlet and symplectic Euler, anti-clockwise for the implicit midpoint rule. The same behaviour occurs for the exact solution of *perturbed* Kepler problems (Exercise 12) and has occupied astronomers for centuries.

Our next experiment (Fig. 2.3) studies the conservation of invariants and the global error. The main observation is that the error in the energy grows linearly for the explicit Euler method, and it remains bounded and small (no secular terms) for the symplectic Euler method. The global error, measured in the Euclidean norm, shows a quadratic growth for the explicit Euler compared to a linear growth for the symplectic Euler. As indicated in Table 2.1 the implicit midpoint rule and the Störmer–Verlet scheme behave similar to the symplectic Euler, but have a smaller

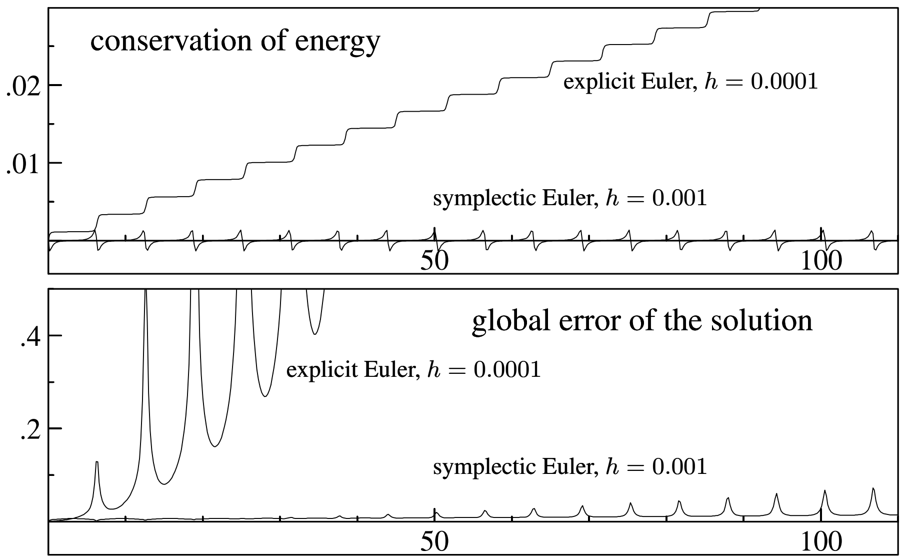

Fig. 2.3. Energy conservation and global error for the Kepler problem

Table 2.1. Qualitative long-time behaviour for the Kepler problem; t is time, h the step size

method	error in H	error in L	global error
explicit Euler	$\mathcal{O}(th)$	$\mathcal{O}(th)$	$\mathcal{O}(t^2h)$
symplectic Euler	$\mathcal{O}(h)$	0	$\mathcal{O}(th)$
implicit midpoint	$\mathcal{O}(h^2)$	0	$\mathcal{O}(th^2)$
Störmer–Verlet	$\mathcal{O}(h^2)$	0	$\mathcal{O}(th^2)$

error due to their higher order. We remark that the angular momentum $L(p,q)$ is exactly conserved by the symplectic Euler, the Störmer–Verlet, and the implicit midpoint rule.

I.2.4 The Outer Solar System

> The evolution of the entire planetary system has been numerically integrated for a time span of nearly 100 million years[5]. This calculation confirms that the evolution of the solar system as a whole is chaotic, . . .
>
> (G.J. Sussman & J. Wisdom 1992)

We next apply our methods to the system which describes the motion of the five outer planets relative to the sun. This system has been studied extensively by astronomers. The problem is a Hamiltonian system (1.10) (N-body problem) with

$$H(p,q) = \frac{1}{2}\sum_{i=0}^{5} \frac{1}{m_i}\, p_i^T p_i - G \sum_{i=1}^{5}\sum_{j=0}^{i-1} \frac{m_i\, m_j}{\|q_i - q_j\|}. \qquad (2.12)$$

Here p and q are the supervectors composed by the vectors $p_i, q_i \in \mathbb{R}^3$ (momenta and positions), respectively. The chosen units are: masses relative to the sun, so that the sun has mass 1. We have taken

$$m_0 = 1.00000597682$$

to take account of the inner planets. Distances are in astronomical units (1 [A.U.] = 149 597 870 [km]), times in earth days, and the gravitational constant is

$$G = 2.95912208286 \cdot 10^{-4}.$$

The initial values for the sun are taken as $q_0(0) = (0,0,0)^T$ and $\dot q_0(0) = (0,0,0)^T$. All other data (masses of the planets and the initial positions and initial velocities) are given in Table 2.2. The initial data is taken from “Ahnerts Kalender für Sternfreunde 1994”, Johann Ambrosius Barth Verlag 1993, and they correspond to September 5, 1994 at 0h00.[6]

[5] 100 million years is not much in astronomical time scales; it just goes back to “Jurassic Park”.

[6] We thank Alexander Ostermann, who provided us with this data.

Table 2.2. Data for the outer solar system

planet	mass	initial position	initial velocity
Jupiter	$m_1 = 0.000954786104043$	-3.5023653 -3.8169847 -1.5507963	0.00565429 -0.00412490 -0.00190589
Saturn	$m_2 = 0.000285583733151$	9.0755314 -3.0458353 -1.6483708	0.00168318 0.00483525 0.00192462
Uranus	$m_3 = 0.0000437273164546$	8.3101420 -16.2901086 -7.2521278	0.00354178 0.00137102 0.00055029
Neptune	$m_4 = 0.0000517759138449$	11.4707666 -25.7294829 -10.8169456	0.00288930 0.00114527 0.00039677
Pluto	$m_5 = 1/(1.3 \cdot 10^8)$	-15.5387357 -25.2225594 -3.1902382	0.00276725 -0.00170702 -0.00136504

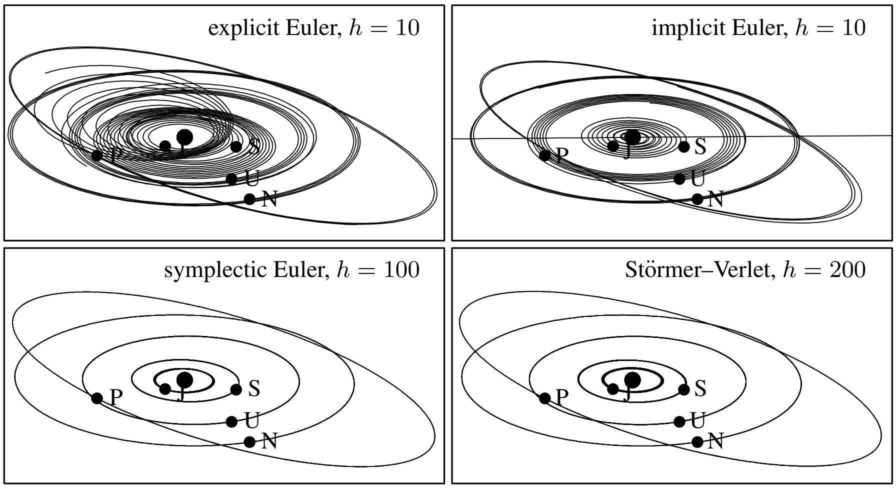

Fig. 2.4. Solutions of the outer solar system

To this system we apply the explicit and implicit Euler methods with step size $h = 10$, the symplectic Euler and the Störmer–Verlet method with much larger step sizes $h = 100$ and $h = 200$, repectively, all over a time period of $200\,000$ days. The numerical solution (see Fig. 2.4) behaves similarly to that for the Kepler problem. With the explicit Euler method the planets have increasing energy, they spiral outwards, Jupiter approaches Saturn which leaves the plane of the two-body motion. With the implicit Euler method the planets (first Jupiter and then Saturn)